Spatial Narrowing of Two-Photon Imaging in a Silicon CCD Camera

Wei Liu, Dongyi Shen, Guolin Zhao, Hengzhe Yan, Zhihao Zhou, and Wenjie Wan

***Abstract*— Imaging based on nonlinear two-photon absorption can offer an attractive alternative for the traditional one-photon imaging scheme with many potential benefits of imaging resolution, speed, and ability to image through scattering media. Here we experimentally demonstrate a direct imaging scheme based on two-photon absorption in the conventional silicon CCD camera and observe a spatial narrowing effect in its imaging. This technique, compared with its one-photon counterpart, exhibits a better imaging resolution and signal-to-noise ratio, thanks to the nonlinear nature of the two-photon absorption process. This nonlinear imaging scheme opens up an avenue for rapid real-time and high-resolution imaging through scattering media like rain, fog, and biomedical samples.**

***Index Terms*— Nonlinear optics, optical imaging, image enhancement, infrared imaging.**

I. Introduction

TWO-PHOTON absorption (TPA) imaging has attracted many interests across many disciplines such as biology, medical science, materials, and nanotechnology [1]–[4]. TPA inherently is a nonlinear process in which a transition from a ground state to an excited state is achieved by simultaneously absorbing two photons. This enables a unique microscopic technique, i.e. two-photon fluorescence microscopy [1], permitting deeper penetration and better three-dimensional resolution in complex bio-samples [5]. Recently, TPA has been explored for its nonlinear response with sub-bandgap excitations in semiconductors, especially in photodetectors [6]–[8]. Unlike other optical nonlinear processes in crystals, e.g. second harmonic, Kerr effect, TPA in semiconductors can be ultrafast in time gating [7], insensitive to temporal phase varying and polarization [9], offering a unique opportunity for imaging purposes [9]. For example, TPA imaging similar to optical coherent tomography (OCT) configuration [10] has been demonstrated to be insensitivity to temporal and spatial turbulence [9], which is finally be utilized for imaging through an opaque scattering medium [11]. Moreover, three-dimensional mid-IR imaging [12] can be obtained using nondegenerate TPA with an uncooled GaN photodiode with an efficiency comparable to traditional liquid-nitrogen-cooled HgCdTe (MCT) detectors [8], where the nondegenerate TPA allows expanding the detection spectrum into mid-IR range [13] with enhanced sensitivity [8].

Manuscript received November 22, 2021; revised March 14, 2022; accepted March 30, 2022. Date of publication April 4, 2022; date of current version April 18, 2022. This work was supported by the National Natural Science Foundation of China under Grant 92050113, Grant 11304201, and Grant 11674228. *(Corresponding author: Wenjie Wan.)*

The authors are with the School of Physics and Astronomy, Shanghai Jiao Tong University, Shanghai 200240, China, and also with the University of Michigan-Shanghai Jiao Tong University Joint Institute, Shanghai Jiao Tong University, Shanghai 200240, China (e-mail: wenjie.wan@sjtu.edu.cn).

Color versions of one or more figures in this letter are available at https://doi.org/10.1109/LPT.2022.3164462.

Digital Object Identifier 10.1109/LPT.2022.3164462

Although these features of TPA imaging may be crucial in many areas, their practical applications are halted by imaging speed mainly due to the raster scanning process associated with the single-detector imaging scheme. This problem can be overcome by incorporating TPA imaging with commercially available imaging array detectors such as charge-coupled devices (CCD), CMOS [14]–[17], where silicon materials also permit TPA processes [18]. In this manner, such silicon-based cameras detour the problem of scanning in TPA imaging, offering a fast, affordable, and efficient alternative TPA imaging scheme in visible, near-IR, extendable to mid-IR spectrum. Previously, using this technique, single-shot recording of an ultrashort laser pulse sonogram has been achieved in a conventional silicon CCD camera [14]; Similarly, wide-field mid-IR images for chemically selective imaging of polymers and biological samples have been demonstrated at 100 ms exposure times using picosecond pulse through non-degenerate TPA, also in a standard Si-based CCD [15]; Moreover, this technique can be further improved to realize rapidly wide-field, high-definition 3D tomographic imaging with chemical selectivity of structured materials and biological samples [16].

In the letter, we experimentally demonstrate TPA imaging with an enhanced resolution as compared to the one-photon detection in a conventional silicon CCD camera, where sub-bandgap photons can be up-converted through TPA and form images. The enhanced resolution origins from the quadratic dependence of the excitation intensity during TPA, as a result, the widths of measured spatial beam profiles by TPA are effectively reduced from its one-photon counterpart. Furthermore, this effect permits an enhanced TPA imaging scheme against scattering background, which inherently provides a better resolution and signal-to-noise ratio to the traditional one-photon imaging technique. This nonlinear imaging technique allows rapid real-time and high-resolution imaging without time-consuming scanning and paves the way for practical imaging applications through scattering media in free-space, underwater, biomedical areas.

II. Theory and Method

In traditional imaging techniques, signals in the detectors scale linearly with incident optical intensity. In contrast, two-photon absorption is an inherently nonlinear process through simultaneously absorbing two sub-bandgap photons and promoting one electron to the conduction band (Fig. 1), as a result, the TPA signals scale quadratically with the excitation optical intensity at photon energy below the bandgap as:

$$S_{TPA} = \beta \frac{P^2}{s} \tag{1}$$

where S_{TPA} represents a two-photon signal, β is TPA efficiency, P is incident power and s is the spot area. Equation (1)

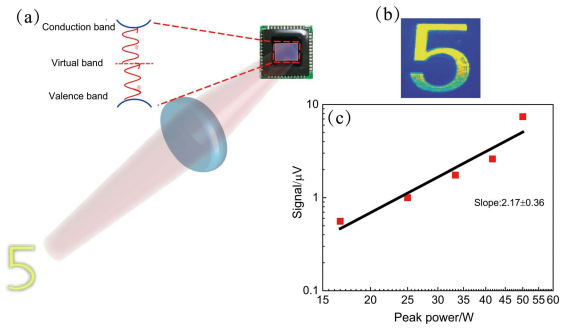

Fig. 1. The principle of two-photon absorption imaging on a conventional silicon CCD camera. (a) simple optical setup imaging through two-photon absorption. The inset is the two-photon process in which the valence band absorbs one photon (reference) to a virtual state, subsequently absorbs another photon (signal) to the conduction band, and produces a photocurrent. (b)image of target "5" from USFA resolution test on a conventional silicon CCD camera with 1550nm laser. (c) the signal response of two-photon absorption to 1550nm laser with a silicon avalanche photodetector (APD) combining a lock-in amplifier, and its slope is 2.17.

shows that the TPA signal not only depends on the square of input power but also is inversely proportional to spot area. In this manner, such TPA detectors offer a unique way to image sub-bandgap photons in a quadratic response, unlike the linear response with the traditional one-photon detection. This feature enables us a unique way to enhance imaging resolution, especially through a scattering medium, as we shall discuss in the following section.

For an optical imaging system, imaging resolution is crucial. Conventionally, image formation in the imaging system could be generally described by using the image of a point, namely the point spread function (PSF). The image of an object is obtained by convolving the object intensity distribution with the PSF. Assuming the original PSF of the optical system can be approximated by a 3D Gaussian distribution, in a conventional one-photon CCD, i.e. $P_0 \exp(-\frac{x^2+y^2}{2\omega_0^2} - \frac{z^2}{2\omega_{0z}^2})$ where P_0 is the initial power at the origin, ω_0 and ω_{0z} are the width in the transverse and axial directions. According to Eq. 1, the TPA signal is the square of optical power and is in the inverse ratio of spot area, and it is written with (2). The attribute of two-photon absorption with a beam pump laser is different from up-conversion two-photon absorption [19] in which signals depend on linearly the optical intensity. Equation (2) shows that the width of the "new" PSF is shrunk by $\sqrt{2}$ times along all three dimensions and the imaging resolution is improved by a factor of $\sqrt{2}$, i.e. $\tilde{\omega}_0 = \omega_0 \Big/ \sqrt{2}$ and $\tilde{\omega}_{0z} = \omega_{0z} \Big/ \sqrt{2}$:

$$S_{TPA} = \beta P_0^2 \exp\left(-\frac{x^2+y^2}{2\tilde{\omega}_0^2} - \frac{z^2}{2\tilde{\omega}_{0z}^2}\right)/s \qquad (2)$$

Such resolution enhancement of TPA imaging is theoretically much similar to prior works in high-order correlation imaging [20]–[22], which, however, requires temporal fluctuations/modulations of the imaging signal, while TPA imaging provides an instant and real-time technique for imaging. Moreover, the sub-bandgap photons with a longer wavelength are believed to have better immunity against scattering events [23], these combined features pave a way for some practical imaging applications through scattering media.

III. Results

Experimentally, we implement a TPA imaging configuration to verify the above theory, using a 120 femtosecond laser (ErFemto-780 Pro) at the wavelength of 1550nm as the signal beam whose TPA efficiency is high for silicon, and a conventional silicon CCD camera (QHY 5L-II-M) as a TPA imaging sensor in Figure 1. Fig. 1(a) shows the general schematics of TPA imaging with a signal beam at 1550nm (below silicon's bandgap photon ~1100nm) directly impinged onto a silicon CCD camera where TPA occurs. During the TPA process, pixels in the CCD allow absorbing one photon to pump an electron to an intermediate virtual state, followed by absorbing a secondary cascaded photon to promote the electron to the final conduction band.

As a result, TPA signals can be generated in each active pixel to form an image, such that the imaging object "5" from the USFA resolution card is imaged at the CCD with the 1550nm laser as shown in Fig. 1(b). To illustrate the nature of TPA, we perform an additional measurement of TPA signals with respect to the input laser power as shown in Fig. 1(c): the quadratic dependence exhibits a slope rate around 2.17 in the log-scale plot, well predicted by the theoretical relation shown in (1).

To evaluate the resolution enhancement predicted by (2), we have experimentally compared images of the spot by using Si CCD and InGaAs CCD (NIRvana, 640). Fig. 2(a) and (b) show the spatial profiles of a 1550nm laser beam. The images in Fig. 2(a) and 2(b) are normalized by the resolution target. Compared with Fig. 2(a), Fig. 2(b) exhibits a clear spatial narrowing effect, and its narrowing ratio is 1.2 which is close to the theoretical result $\sqrt{2}$. Besides, we also compare the spatial profiles, e.g. Full-Width Half-Maximum (FWHM) of one signal beam at its focus, separately using a one-photon detector (InGaAs APD, Thorlabs-APD 130C/M) and a TPA one (silicon APD, Thorlabs-APD 120A/M). Fig. 2(c) and (d) show the spatial profiles of a 1550nm laser beam along the transverse (x) and the axial (z) directions with the two type detectors. Obviously, the transverse profiles read by TPA detectors exhibit narrower FWHMs than its counterpart by the one-photon detector, and the ratio of the FWHMs with the two type detectors is ~3. To demonstrate the narrowing effect along the axial direction, we purposely focus down the laser and scan its focal spot using the two detectors, here the ratio between the FWHMs further enlarge to 10. These results exceed the theoretical narrowing value of $\sqrt{2}$ predicted from (2). We believe this observation may origin from two aspects: first, TPA signals inversely depend on the spot size as indicated by (2), although we tend to control the aperture size uniform in all our measurements, the diverge angle in different regimes of the laser spot may cause some variant in TPA detections; second, if the incident 1550nm laser is too weak to generate TPA signal, i.e. down to background noise level, we cannot obtain any spatial profile distribution, meanwhile, one-photon detectors would not suffer the same problem. Effectively, such low responsivity of TPA detection further shrinks the measured FWHMs. Besides, the effect is enhanced by using high NA objective lens.

Nevertheless, this narrowing effect using TPA detection suggests one important implication in imaging applications to enhance the resolution, especially helpful for imaging through

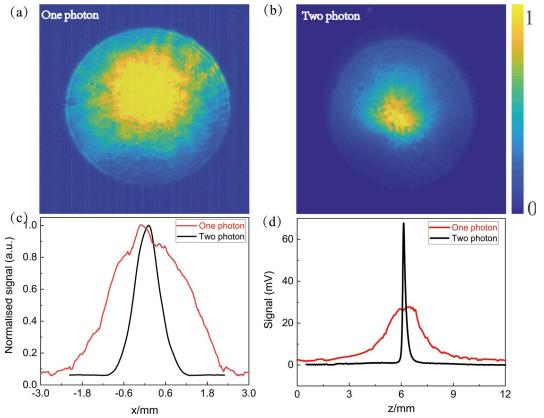

Fig. 2. Spatial profiles measured through one-photon absorption and two-photon absorption using a 1550nm laser source, Si CCD, InGaAs CCD, a silicon APD (Thorlabs, APD 120A/M) as a two-photon detector, and an InGaAs APD (Thorlabs, APD 130C/M) as a one-photon detector. The spot diameter from the 1550nm laser is ∼5mm. (a) spot image using InGaAs CCD; (b)spot image using Si CCD; (c) x-direction profiles. We place a slit before the objective lens and move the slit from the left to right along the x-direction; (d) z-direction profiles by moving the objective lens along the z-direction.

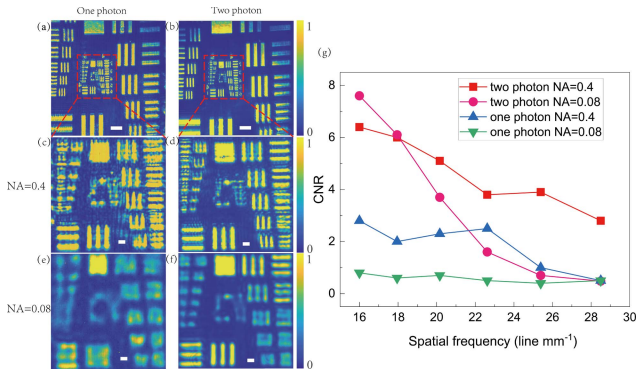

Fig. 3. The images of resolution target one-photon absorption and two-photon absorption using a 1550nm laser source in Si CCD and InGaAs CCD. (a)one-photon image using an InGaAs CCD; (b) two-photon image using a Si CCD; The scale bar is 250μm in Fig 3a and Fig 3b; (c) zoom-in image of Fig 3a with an effective NA of 0.4; (d) zoom-in image of Fig 3b with an effective NA of 0.4; (e) zoom-in image of Fig 3a with an effective NA of 0.08; (d) zoom-in image of Fig 3b with an effective NA of 0.08; The scale bar is 150μm in Fig 3c-f; (g) The CNRs from the images are plotted as a function of spatial frequency.

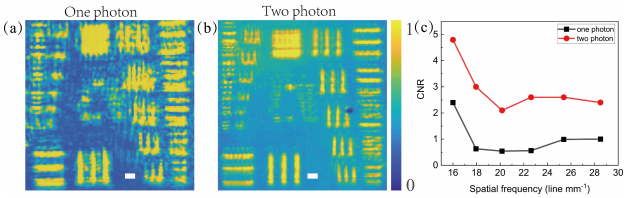

Fig. 4. Images through a rotating ground glass using a 1550nm laser in a Si CCD and an InGaAs CCD. (a)one-photon image using an InGaAs CCD; (b)two-photon image using a Si CDD; The scale bar 150μm. (c) The CNRs from the images are plotted as a function of spatial frequency.

scattering media. It is well-known that PSF that propagates through a scattering medium would be broadened due to scattering events, which finally leads to a blurred image. Previously, with the help of a secondary reference beam, ballistic photons that don't suffer any scattering can be distinguished out using a single TPA detector, such that, images can be scanned and reconstructed even through an opaque and dynamical scattering medium [11]. Moreover, high-order correlations have also been explored to enhance fluorescent microscopy [21], even with the second-order correlations [24]. With the current observation in Fig. 2 and theoretical prediction in (2), we believe such narrowing effect of TPA imaging may also be implemented to enhance the imaging resolution through a scattering medium, where the narrowing may behave like a spatial filter to enhance the high-intensity portion in the images while suppressing others with low intensity such as scattered lights.

To demonstrate directly two-photon absorption narrowing effect, we implement one-photon imaging and two-photon imaging with an InGaAs CCD and a silicon CCD using a 120 femtosecond laser at 1550nm. The imaging object, i.e. a resolution card, can be illuminated with a laser source at 1550nm, the laser beam transmits and converges through an objective lens onto the two kinds of CCD cameras separately. Figure 3 shows the images of the resolution card. Although the clear images are both exhibited in Fig. 3(a) and Fig. 3(b), the image of zooming in Fig. 3(b) is clearer than the one of zooming in Fig. 3(a). The one reason is the two-photon narrowing effect, and the other reason is the signal-to-noise ratio (SNR) of one-photon absorption is I_{signal}/I_{noise}, where I_{signal} is the intensity of signal and I_{noise} is the intensity of noise mainly caused by the scattering light, meanwhile, SNR of TPA indeed is the square of SNR of one-photon absorption, $(I_{signal}/I_{noise})^2$. Moreover, to show clearly the two-photon absorption narrowing effect, we decrease the effective NA of the objective lens by reducing the entrance pupil diameter with a pinhole. The results are shown in Fig. 3(e) and (f). Obviously, the resolution of Fig 3(e) is higher than the resolution of Fig 3(f). Here image quality can be compared quantitatively using the contrast-to-noise ratio (CNR) which is defined as $(\langle I_f\rangle - \langle I_b\rangle)/((\sigma_f + \sigma_b)/2)$, where $\langle I_f\rangle$ is the average intensity of the feature of interest, $\langle I_b\rangle$ is the average intensity of the surrounding background, and σ is the standard deviation of pixel intensity. From Fig 3(g), CNRs of all images decrease, but CNRs of two-photon images are higher than one of the one-photon images. Therefore, two-photon absorption possesses a spatial narrowing effect for imaging applications.

To validate this technique's potential application in scattering imaging, we implement TPA imaging with a silicon CCD for imaging through a scattering medium, i.e. a rotating ground glass. As shown in Figure 5, the imaging object, i.e. a resolution card, can be illuminated with a laser source at 1550nm, the laser beam transmits through a rotating ground glass (single scattering layer), and converges through an objective lens onto the silicon CCD camera. Figure 4 shows images using a Si CCD and an InGaAs CCD. Compared with Fig. 3(c) and Fig. 3(d), the resolution of images in Fig. 4(a) and 4(b) both declines. However, the resolution of the two-photon image is better than its one-photon counterpart. To compare one- and two-photon images quantitatively, the CNR is shown in Fig. 4(c). From Fig. 4(c), CNRs of all images decrease, but CNRs of the two-photon images are higher than their one-photon counterpart. Therefore, two-photon absorption resists crosstalk that produces speckle.

To further exam the spatial narrowing effect in the axial direction, we move the CCD camera along the axial direction to observe the evolution of imaging patterns as shown in Fig. 5. The aforementioned narrowing effect in the beam's spatial profiles can manifest itself here in two ways: along the

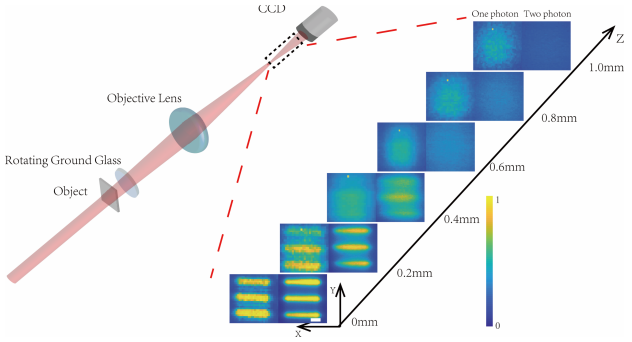

Fig. 5. The experimental setup of imaging through a rotating ground glass (Thorlabs, DG20-220) using a 1550nm laser in a Si CCD and an InGaAs CCD, and images along z-direction by moving the objective lens. The scale bar 200μm.

axial direction, we observe the TPA imaging are more limited to its focal point near 0mm, and quickly diminishes around the distance of 0.6mm away from the focus. In contrast, the one-photon imaging spans across a much wider range up to 1mm, even when the image becomes blurred. This observation is in line with the previous results in Fig. 2. More importantly, the resolution of TPA imaging is much enhanced compared to its counterpart at the same distance, where the one-photon images are always in company with some low-intensity background from scattering. For example, the image at 0.4mm by TPA is still distinguishable, but the other one by one-photon absorption is fully blurred. On the one hand, this enhancement is contributed by the nonlinear intensity dependence mentioned above. On the other hand, according to the definition of signal-to-noise ratio (SNR), SNR of one-photon absorption is I_{signal}/I_{noise}, where I_{signal} is the intensity of signal and I_{noise} is the intensity of noise mainly caused by the scattering light, meanwhile, SNR of TPA indeed is the square of SNR of one-photon absorption, $(I_{signal}/I_{noise})^2$. Compared with SNR of one-photon absorption, SNR of two-photon absorption is higher.

IV. Conclusion

In conclusion, we have experimentally demonstrated the imaging through a scattering medium using a sub-bandgap infrared femtosecond laser in a conventional silicon CCD camera. Compared with the one-photon absorption detected profile, the FWHM of spatial profiles through TPA is greatly shrunk, providing us a door to realize imaging with an enhanced resolution, even though a scattering medium. As compared to other existing enhanced resolution imaging techniques, imaging in a conventional silicon CCD with TPA exhibits several advantages, such as label-free, wide-field and high-resolution imaging. Moreover, it is suitable for rapid imaging without raster scanning as compared to other enhanced resolution imaging techniques using nonlinearly wave mixing [25], synthetic aperture [26]. Although efficiency and wavelength range of TPA are limitations, this technique opens up a new avenue for rapid infrared imaging in the biomedical area.

References

[1] W. Denk, J. H. Strickler, and W. W. Webb, "Two-photon laser scanning fluorescence microscopy," *Science*, vol. 248, no. 4951, pp. 73–76, Apr. 1990.

[2] M. Drobizhev, N. S. Makarov, S. E. Tillo, T. E. Hughes, and A. Rebane, "Two-photon absorption properties of fluorescent proteins," *Nature Methods*, vol. 8, no. 5, pp. 393–399, Apr. 2011.

[3] G. S. He, L.-S. Tan, Q. Zheng, and P. N. Prasad, "Multiphoton absorbing materials: Molecular designs, characterizations, and applications," *Chem. Rev.*, vol. 108, no. 4, pp. 1245–1330, Mar. 2008.

[4] M. Farsari and B. N. Chichkov, "Two-photon fabrication," *Nature Photon.*, vol. 3, no. 8, pp. 450–452, Aug. 2009.

[5] F. Helmchen and W. Denk, "Deep tissue two-photon microscopy," *Nature Methods*, vol. 2, no. 12, pp. 932–940, Nov. 2005.

[6] J. M. Roth, T. E. Murphy, and C. Xu, "Ultrasensitive and high-dynamic-range two-photon absorption in a GaAs photomultiplier tube," *Opt. Lett.*, vol. 27, no. 23, pp. 2076–2078, Dec. 2002.

[7] F. Boitier, A. Godard, E. Rosencher, and C. Fabre, "Measuring photon bunching at ultrashort timescale by two-photon absorption in semiconductors," *Nature Phys.*, vol. 5, no. 4, pp. 267–270, Mar. 2009.

[8] D. A. Fishman *et al.*, "Sensitive mid-infrared detection in wide-bandgap semiconductors using extreme non-degenerate two-photon absorption," *Nature Photon.*, vol. 5, no. 9, pp. 561–565, Aug. 2011.

[9] A. Nevet, T. Michaeli, and M. Orenstein, "Second-order optical coherence tomography: Deeper and turbulence-free imaging," *J. Opt. Soc. Amer. B, Opt. Phys.*, vol. 30, no. 2, pp. 258–265, Jan. 2013.

[10] D. Huang *et al.*, "Optical coherence tomography," *Science*, vol. 254, no. 5035, pp. 1178–1181, Nov. 1991.

[11] W. Liu *et al.*, "Imaging through dynamical scattering media by two-photon absorption detectors," *Opt. Exp.*, vol. 29, no. 19, pp. 29972–29981, Sep. 2021.

[12] H. S. Pattanaik, M. Reichert, D. J. Hagan, and E. W. Van Stryland, "Three-dimensional IR imaging with uncooled GaN photodiodes using nondegenerate two-photon absorption," *Opt. Exp.*, vol. 24, no. 2, pp. 1196–1205, Jan. 2016.

[13] G. Xu *et al.*, "Sensitive infrared photon counting detection by nondegenerate two-photon absorption in Si APD," *IEEE Photon. Technol. Lett.*, vol. 31, no. 24, pp. 1944–1947, Dec. 15, 2019.

[14] D. Panasenko and Y. Fainman, "Single-shot sonogram generation for femtosecond laser pulse diagnostics by use of two-photon absorption in a silicon CCD camera," *Opt. Lett.*, vol. 27, no. 16, pp. 1475–1477, Aug. 2002.

[15] D. Knez, A. M. Hanninen, R. C. Prince, E. O. Potma, and D. A. Fishman, "Infrared chemical imaging through non-degenerate two-photon absorption in silicon-based cameras," *Light, Sci. Appl.*, vol. 9, no. 1, pp. 1–10, Jul. 2020.

[16] E. O. Potma *et al.*, "Rapid chemically selective 3D imaging in the mid-infrared," *Optica*, vol. 8, no. 7, pp. 995–1002, Jul. 2021.

[17] J. Fang, Y. Wang, E. Wu, M. Yan, K. Huang, and H. Zeng, "Single-photon infrared imaging with a silicon camera based on long-wavelength-pumping two-photon absorption," *IEEE J. Sel. Topics Quantum Electron.*, vol. 28, no. 2, pp. 1–7, Mar. 2022.

[18] A. D. Bristow, N. Rotenberg, and H. M. van Driel, "Two-photon absorption and Kerr coefficients of silicon for 850–2200 nm," *Appl. Phys. Lett*, vol. 90, no. 19, pp. 191104–191106, Mar. 2007.

[19] F. Boitier, J.-B. Dherbecourt, A. Godard, and E. Rosencher, "Infrared quantum counting by nondegenerate two photon conductivity in GaAs," *Appl. Phys. Lett.*, vol. 94, no. 8, pp. 81112–81114, Dec. 2009.

[20] T. Dertinger, R. Colyer, G. Iyer, S. Weiss, and J. Enderlein, "Fast, background-free, 3D super-resolution optical fluctuation imaging (SOFI)," *Proc. Nat. Acad. Sci. USA*, vol. 106, no. 52, pp. 22287–22292, Dec. 2009.

[21] Y. Liu, L. Chen, W. Liu, X. Liang, and W. Wan, "Resolution-enhanced imaging through scattering media by high-order correlation," *Appl. Opt.*, vol. 58, no. 9, pp. 2350–2357, Mar. 2019.

[22] X. Sunian *et al.*, "Resolution enhanced photothermal imaging by high-order correlation," *Opt. Lett.*, vol. 45, no. 20, pp. 5696–5699, Oct. 2020.

[23] N. M. Israelsen *et al.*, "Real-time high-resolution mid-infrared optical coherence tomography," *Light, Sci. Appl.*, vol. 8, no. 1, pp. 11–13, Jan. 2019.

[24] J.-E. Oh, Y.-W. Cho, G. Scarcelli, and Y.-H. Kim, "Sub-Rayleigh imaging via speckle illumination," *Opt. Lett.*, vol. 38, no. 5, pp. 682–684, Mar. 2013.

[25] Z. Zhou *et al.*, "Far-field super-resolution imaging by nonlinearly excited evanescent waves," *Adv. Photon.*, vol. 3, no. 2, Apr. 2021, Art. no. 025001.

[26] C. Zheng *et al.*, "High spatial and temporal resolution synthetic aperture phase microscopy," *Adv. Photon.*, vol. 2, no. 6, Nov. 2020, Art. no. 065002.